



# Hard Sample Aware Network for Contrastive Deep Graph Clustering

Jianan Zhao\*  
University of Notre Dame  
Notre Dame, IN, USA  
andy.zhaoja@gmail.com

Qianlong Wen\*  
University of Notre Dame  
Notre Dame, IN, USA  
qwen@nd.edu

Mingxuan Ju  
University of Notre Dame  
Notre Dame, IN, USA  
mju2@nd.edu

Chuxu Zhang<sup>†</sup>  
Brandeis University  
Waltham, MA, USA  
chuxuzhang@brandeis.edu

Yanfang Ye<sup>†</sup>  
University of Notre Dame  
Notre Dame, IN, USA  
yye7@nd.edu

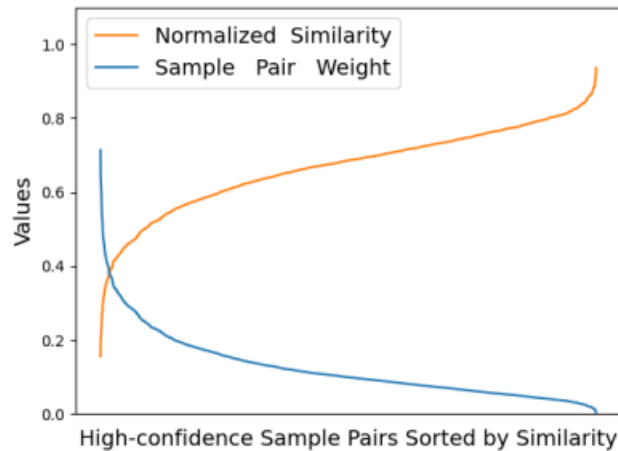
WSDM-2023

Code: <https://github.com/andyjzhao/WSDM23-GSR>

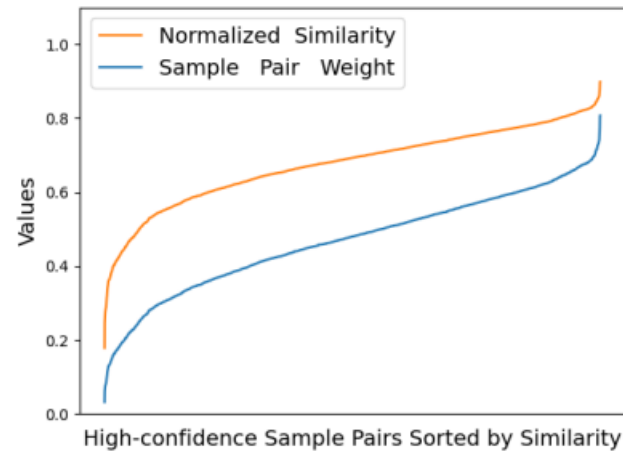


Reported by Dongdong Hu

# Introduction



(a) Positive Sample Pairs



(b) Negative Sample Pairs

1) In the hardness measurement, the important **structural information is overlooked** for similarity calculation, degrading the representativeness of the selected hard negative samples

2) Previous works merely focus on the hard negative sample pairs while **neglecting the hard positive sample pairs**. Nevertheless, samples within the same cluster but with low similarity should also be carefully learned

# Method

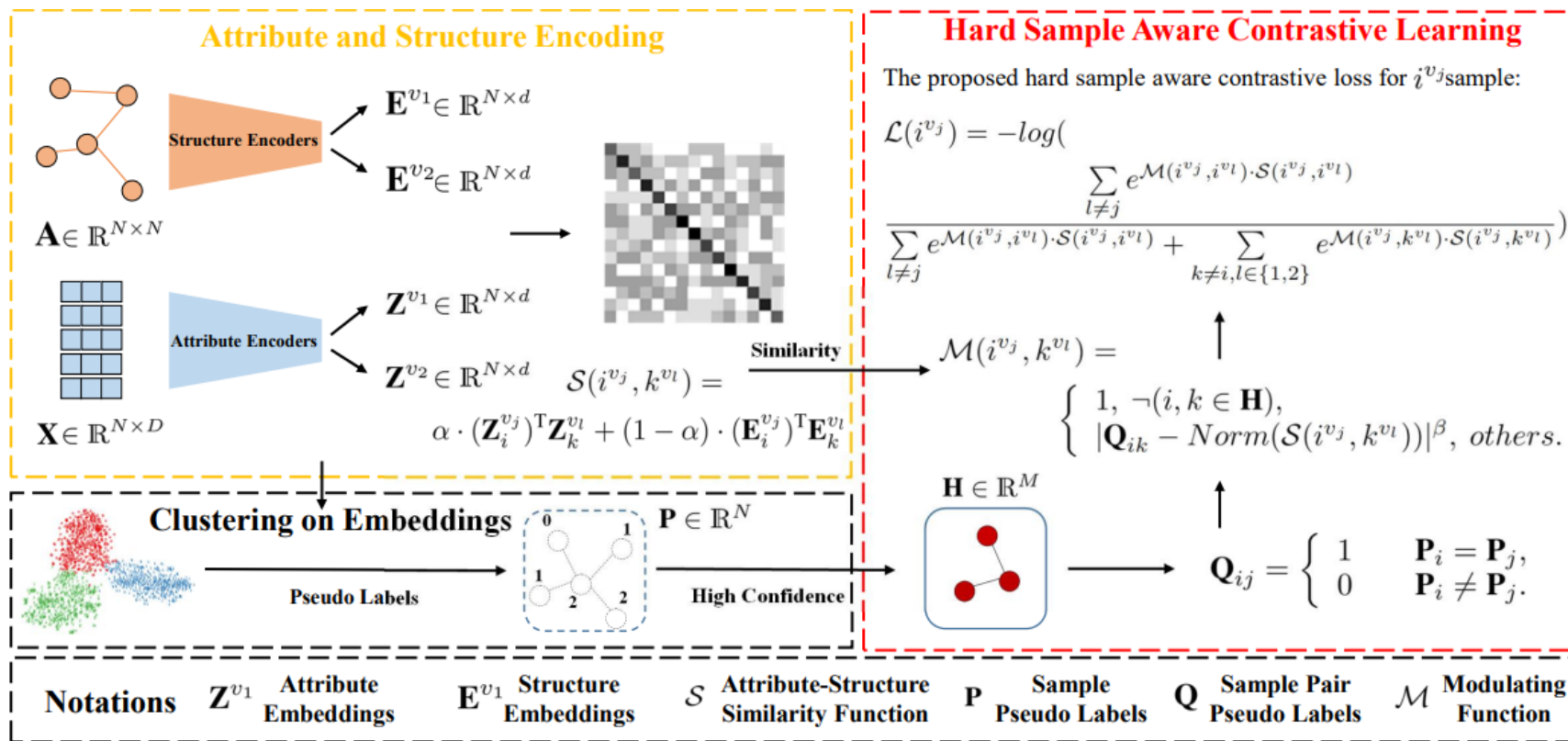
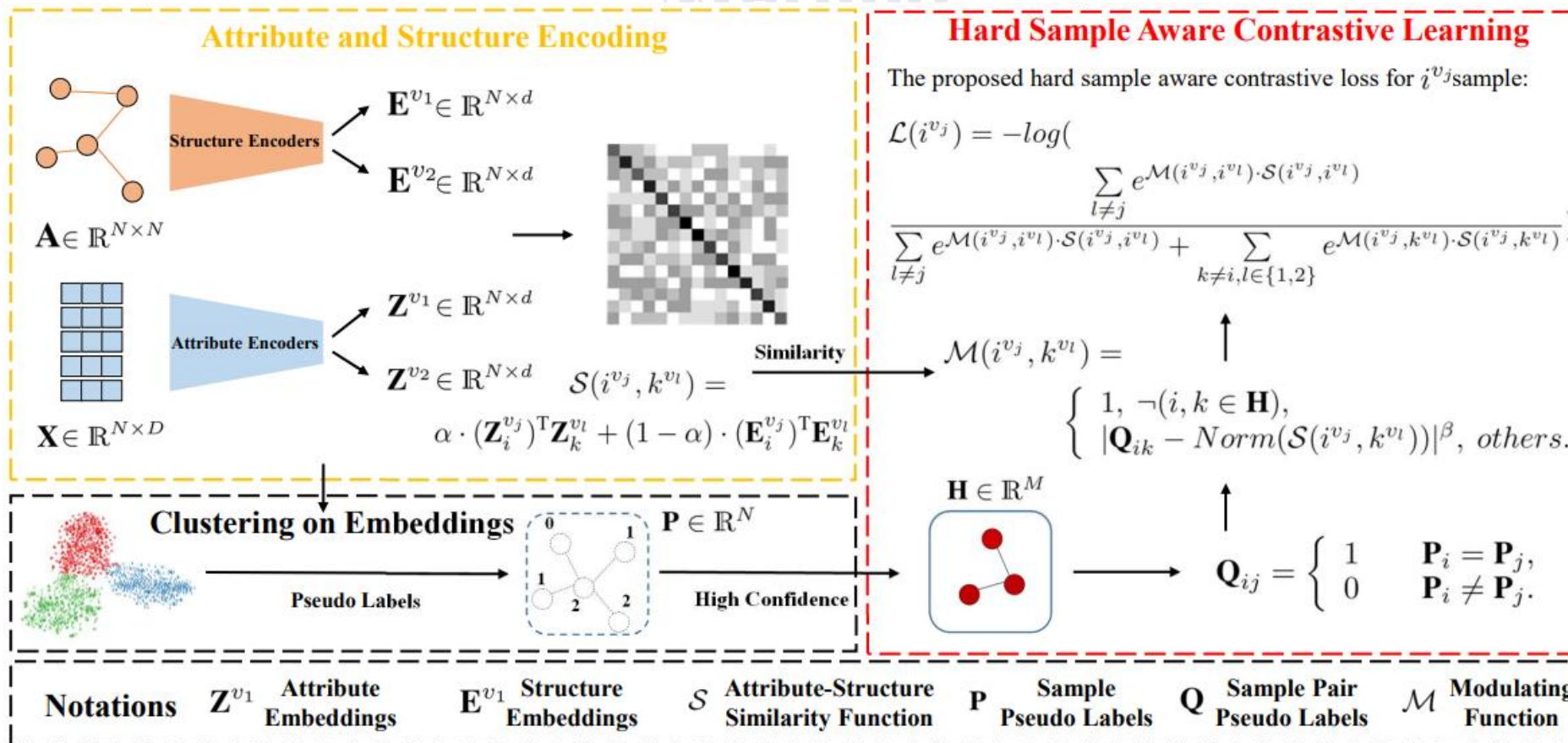


Figure 2: Illustration of our proposed hard sample aware network. In attribute and structure encoding, we embed the attribute and structure into the latent space with the attribute encoders and structure encoders. Then the sample similarities are calculated by a learnable linear combination of attribute similarity and structure similarity, thus better revealing the sample relations. Moreover, guided by the high-confidence information, a general dynamic sample weighting strategy is proposed to up-weight hard sample pairs while down-weighting the easy ones. Overall, the hard sample aware contrastive loss guides the network to focus more on both hard positive and negative sample pairs, thus further improving the discriminative capability of samples.

# Method



$$\mathcal{V} = \{v_1, v_2, \dots, v_N\} \quad \mathcal{E} \text{ be a set of edges}$$

$$\mathbf{X} \in \mathbb{R}^{N \times D} \text{ and } \mathbf{A} \in \mathbb{R}^{N \times N} \quad \mathcal{G} = \{\mathbf{X}, \mathbf{A}\}$$

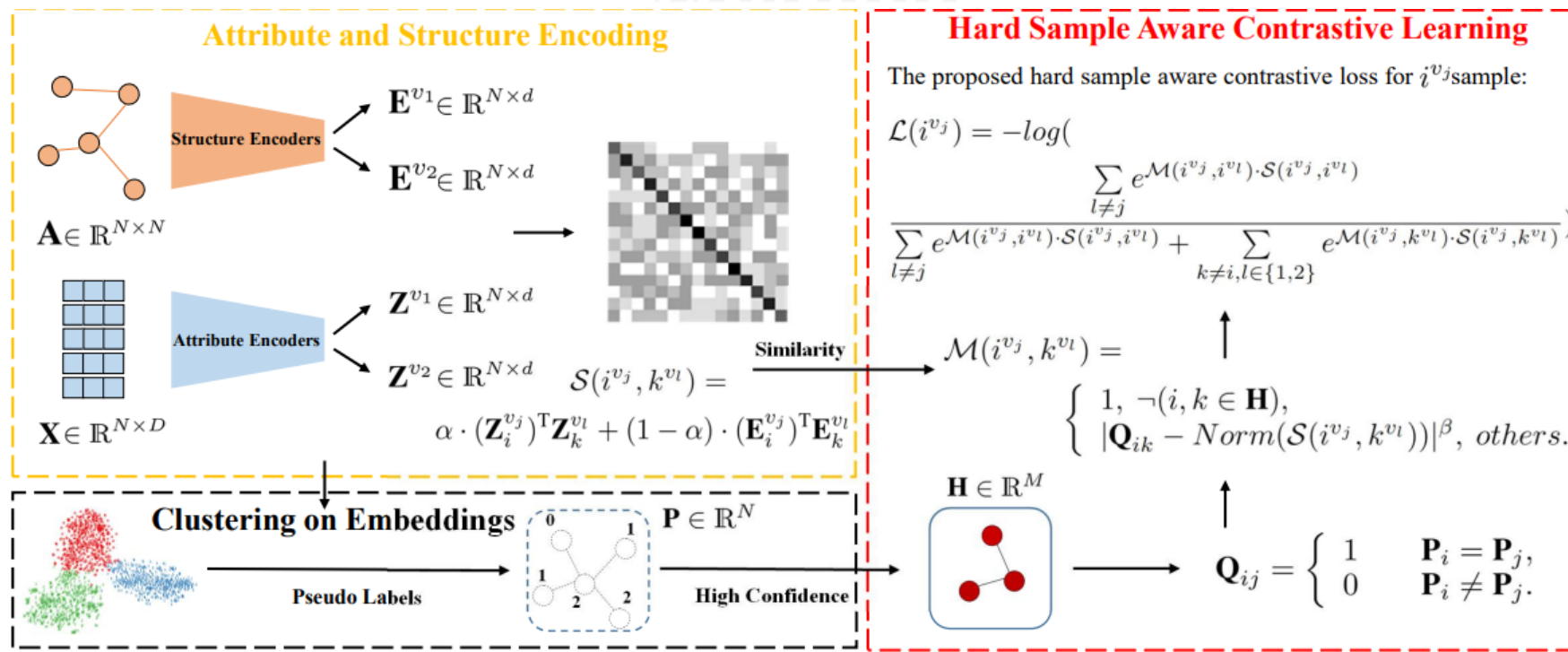
$$\mathbf{D} = \text{diag}(d_1, d_2, \dots, d_N) \in \mathbb{R}^{N \times N}$$

$$\mathbf{E} = \mathcal{F}(\mathbf{A}, \mathbf{X}), \quad (1)$$

$$\Phi = \mathcal{C}(\mathbf{E}), \quad (2)$$

$$\tilde{\mathbf{L}} = \mathbf{I} - \hat{\mathbf{D}}^{-\frac{1}{2}} \hat{\mathbf{A}} \hat{\mathbf{D}}^{-\frac{1}{2}}$$

# Method



$$\tilde{\mathbf{X}} = \left( \prod_{i=1}^t (\mathbf{I} - \tilde{\mathbf{L}}) \right) \mathbf{X} = (\mathbf{I} - \tilde{\mathbf{L}})^t \mathbf{X}, \quad (3)$$

filter the high-frequency noises

$$\mathbf{Z}^{v_1} = \mathbf{A} \mathbf{E}_1(\tilde{\mathbf{X}}); \mathbf{Z}_i^{v_1} = \frac{\mathbf{Z}_i^{v_1}}{\|\mathbf{Z}_i^{v_1}\|_2}, i = 1, 2, \dots, N;$$

$$\mathbf{Z}^{v_2} = \mathbf{A} \mathbf{E}_2(\tilde{\mathbf{X}}); \mathbf{Z}_j^{v_2} = \frac{\mathbf{Z}_j^{v_2}}{\|\mathbf{Z}_j^{v_2}\|_2}, j = 1, 2, \dots, N, \quad (4)$$

where  $\mathbf{Z}^{v_1}$  and  $\mathbf{Z}^{v_2}$  denote two-view attribute embeddings

$$\mathbf{E}^{v_1} = \mathbf{S} \mathbf{E}_1(\mathbf{A}); \mathbf{E}_i^{v_1} = \frac{\mathbf{E}_i^{v_1}}{\|\mathbf{E}_i^{v_1}\|_2}, i = 1, 2, \dots, N;$$

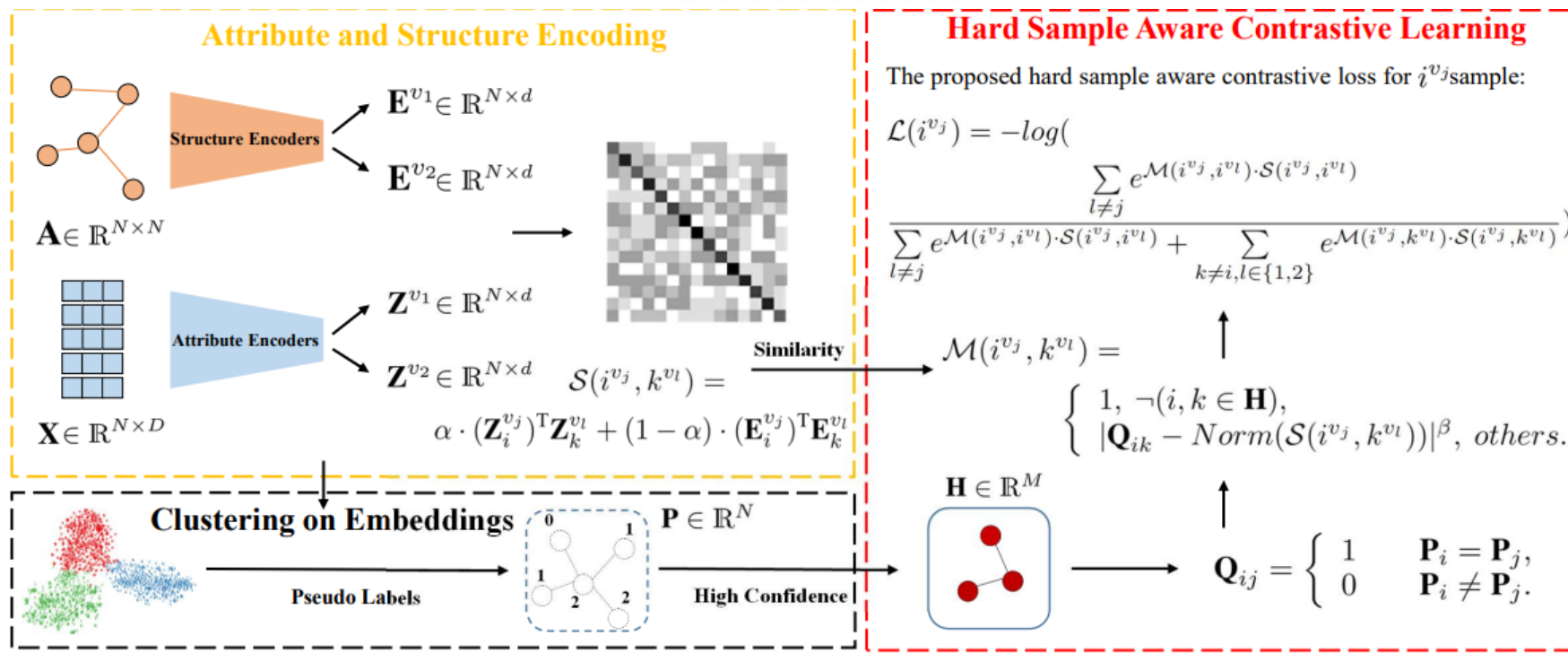
$$\mathbf{E}^{v_2} = \mathbf{S} \mathbf{E}_2(\mathbf{A}); \mathbf{E}_j^{v_2} = \frac{\mathbf{E}_j^{v_2}}{\|\mathbf{E}_j^{v_2}\|_2}, j = 1, 2, \dots, N, \quad (5)$$

$$\mathcal{S}(i^{v_j}, k^{v_l}) = \alpha \cdot (\mathbf{Z}_i^{v_j})^T \mathbf{Z}_k^{v_l} + (1 - \alpha) \cdot (\mathbf{E}_i^{v_j})^T \mathbf{E}_k^{v_l}, \quad (6)$$

where  $i, k \in \{1, 2, \dots, N\}$  and  $j, l \in \{1, 2\}$ .



# Method



$$\mathbf{Q}_{ij} = \begin{cases} 1 & \mathbf{P}_i = \mathbf{P}_j, \\ 0 & \mathbf{P}_i \neq \mathbf{P}_j. \end{cases} \quad (7)$$

$$\mathcal{L}_{infoNCE}(i^{v_j}) = -\log \frac{e^{\theta(i^{v_j}, i^{v_l})}}{e^{\theta(i^{v_j}, i^{v_l})} + \sum_{k \neq i} (e^{\theta(i^{v_j}, k^{v_j})} + e^{\theta(i^{v_j}, k^{v_l})})}. \quad (8)$$

$$\mathcal{L} = \frac{1}{2N} \sum_{j=1}^2 \sum_{i=1}^N \mathcal{L}(i^{v_j}). \quad (11)$$

$$\mathcal{M}(i^{v_j}, k^{v_l}) = \begin{cases} 1, & \neg(i, k \in \mathbf{H}), \\ |\mathbf{Q}_{ik} - Norm(\mathcal{S}(i^{v_j}, k^{v_l}))|^\beta, & \text{others.} \end{cases}$$

1)  $\mathcal{M}$  can up-weight the hard samples while down-weighting the easy samples.

2) The focusing factor  $\beta$  controls the down-weighting rate of easy sample pairs.

# Experiments

Dataset	Metric	Classical Deep Graph Clustering					Contrastive Deep Graph Clustering						Hard Sample Mining		
		MGAE	DAEGC	ARGA	SDCN	DFCN	AGE	MVGRL	AutoSSL	AGC-DRR	DCRN	AFGRL	GDCL	ProGCL	HSAN
		CIKM 19	IJCAI 19	IJCAI 19	WWW 20	AAAI 21	SIGKDD 20	ICML 20	ICLR 22	IJCAI 22	AAAI 22	AAAI 22	IJCAI 21	ICML 22	Ours
CORA	ACC	43.38±2.11	70.43±0.36	71.04±0.25	35.60±2.83	36.33±0.49	<b>73.50±1.83</b>	70.47±3.70	63.81±0.57	40.62±0.55	61.93±0.47	26.25±1.24	70.83±0.47	57.13±1.23	<b>77.07±1.56</b>
	NMI	28.78±2.97	52.89±0.69	51.06±0.52	14.28±1.91	19.36±0.87	<b>57.58±1.42</b>	55.57±1.54	47.62±0.45	18.74±0.73	45.13±1.57	12.36±1.54	56.60±0.36	41.02±1.34	<b>59.21±1.03</b>
	ARI	16.43±1.65	49.63±0.43	47.71±0.33	07.78±3.24	04.67±2.10	<b>50.10±2.14</b>	48.70±3.94	38.92±0.77	14.80±1.64	33.15±0.14	14.32±1.87	48.05±0.72	30.71±2.70	<b>57.52±2.70</b>
	F1	33.48±3.05	68.27±0.57	69.27±0.39	24.37±1.04	26.16±0.50	<b>69.28±1.59</b>	67.15±1.86	56.42±0.21	31.23±0.57	49.50±0.42	30.20±1.15	52.88±0.97	45.68±1.29	<b>75.11±1.40</b>
CITE	ACC	61.35±0.80	64.54±1.39	61.07±0.49	65.96±0.31	69.50±0.20	69.73±0.24	62.83±1.59	66.76±0.67	68.32±1.83	<b>70.86±0.18</b>	31.45±0.54	66.39±0.65	65.92±0.80	<b>71.15±0.80</b>
	NMI	34.63±0.65	36.41±0.86	34.40±0.71	38.71±0.32	43.90±0.20	44.93±0.53	40.69±0.93	40.67±0.84	43.28±1.41	<b>45.86±0.35</b>	15.17±0.47	39.52±0.38	39.59±0.39	<b>45.06±0.74</b>
	ARI	33.55±1.18	37.78±1.24	34.32±0.70	40.17±0.43	45.50±0.30	45.31±0.41	34.18±1.73	38.73±0.55	45.34±2.33	<b>47.64±0.30</b>	14.32±0.78	41.07±0.96	36.16±1.11	<b>47.05±1.12</b>
	F1	57.36±0.82	62.20±1.32	58.23±0.31	63.62±0.24	64.30±0.20	64.45±0.27	59.54±2.17	58.22±0.68	<b>64.82±1.60</b>	<b>65.83±0.21</b>	30.20±0.71	61.12±0.70	57.89±1.98	63.01±1.79
AMAP	ACC	71.57±2.48	75.96±0.23	69.28±2.30	53.44±0.81	<b>76.82±0.23</b>	75.98±0.68	41.07±3.12	54.55±0.97	76.81±1.45		75.51±0.77	43.75±0.78	51.53±0.38	<b>77.02±0.33</b>
	NMI	62.13±2.79	65.25±0.45	58.36±2.76	44.85±0.83	66.23±1.21	65.38±0.61	30.28±3.94	48.56±0.71	<b>66.54±1.24</b>		64.05±0.15	37.32±0.28	39.56±0.39	<b>67.21±0.33</b>
	ARI	48.82±4.57	58.12±0.24	44.18±4.41	31.21±1.23	58.28±0.74	55.89±1.34	18.77±2.34	26.87±0.34	<b>60.15±1.56</b>	OOM	54.45±0.48	21.57±0.51	34.18±0.89	<b>58.01±0.48</b>
	F1	68.08±1.76	69.87±0.54	64.30±1.95	50.66±1.49	71.25±0.31	<b>71.74±0.93</b>	32.88±5.50	54.47±0.83	71.03±0.64		69.99±0.34	38.37±0.29	31.97±0.44	<b>72.03±0.46</b>
BAT	ACC	53.59±2.04	52.67±0.00	<b>67.86±0.80</b>	53.05±4.63	55.73±0.06	56.68±0.76	37.56±0.32	42.43±0.47	47.79±0.02	67.94±1.45	50.92±0.44	45.42±0.54	55.73±0.79	<b>77.15±0.72</b>
	NMI	30.59±2.06	21.43±0.35	<b>49.09±0.54</b>	25.74±5.71	48.77±0.51	36.04±1.54	29.33±0.70	17.84±0.98	19.91±0.24	47.23±0.74	27.55±0.62	31.70±0.42	28.69±0.92	<b>53.21±0.93</b>
	ARI	24.15±1.70	18.18±0.29	<b>42.02±1.21</b>	21.04±4.97	37.76±0.23	26.59±1.83	13.45±0.03	13.11±0.81	14.59±0.13	39.76±0.87	21.89±0.74	19.33±0.57	21.84±1.34	<b>52.20±1.11</b>
	F1	50.83±3.23	52.23±0.03	67.02±1.15	46.45±5.90	50.90±0.12	55.07±0.80	29.64±0.49	34.84±0.15	42.33±0.51	<b>67.40±0.35</b>	46.53±0.57	39.94±0.57	56.08±0.89	<b>77.13±0.76</b>
EAT	ACC	44.61±2.10	36.89±0.15	<b>52.13±0.00</b>	39.07±1.51	49.37±0.19	47.26±0.32	32.88±0.71	31.33±0.52	37.37±0.11	50.88±0.55	37.42±1.24	33.46±0.18	43.36±0.87	<b>56.69±0.34</b>
	NMI	15.60±2.30	05.57±0.06	22.48±1.21	08.83±2.54	<b>32.90±0.41</b>	23.74±0.90	11.72±1.08	07.63±0.85	07.00±0.85	22.01±1.23	11.44±1.41	13.22±0.33	23.93±0.45	<b>33.25±0.44</b>
	ARI	13.40±1.26	05.03±0.08	17.29±0.50	06.31±1.95	<b>23.25±0.18</b>	16.57±0.46	04.68±1.30	02.13±0.67	04.88±0.91	18.13±0.85	06.57±1.73	04.31±0.29	15.03±0.98	<b>26.85±0.59</b>
	F1	43.08±3.26	34.72±0.16	<b>52.75±0.07</b>	33.42±3.10	42.95±0.04	45.54±0.40	25.35±0.75	21.82±0.98	35.20±0.17	47.06±0.66	30.53±1.47	25.02±0.21	42.54±0.45	<b>57.26±0.28</b>
UAT	ACC	48.97±1.52	52.29±0.49	49.31±0.15	52.25±1.91	33.61±0.09	<b>52.37±0.42</b>	44.16±1.38	42.52±0.64	42.64±0.31	49.92±1.25	41.50±0.25	48.70±0.06	45.38±0.58	<b>56.04±0.67</b>
	NMI	20.69±0.98	21.33±0.44	25.44±0.31	21.61±1.26	<b>26.49±0.41</b>	23.64±0.66	21.53±0.94	17.86±0.22	11.15±0.24	24.09±0.53	17.33±0.54	25.10±0.01	22.04±2.23	<b>26.99±2.11</b>
	ARI	18.33±1.79	20.50±0.51	16.57±0.31	21.63±1.49	11.87±0.23	20.39±0.70	17.12±1.46	13.13±0.71	09.50±0.25	17.17±0.69	13.62±0.57	<b>21.76±0.01</b>	14.74±1.99	<b>25.22±1.96</b>
	F1	47.95±1.52	<b>50.33±0.64</b>	50.26±0.16	45.59±3.54	25.79±0.29	50.15±0.73	39.44±2.19	34.94±0.87	35.18±0.32	44.81±0.87	36.52±0.89	45.69±0.08	39.30±1.82	<b>54.20±1.84</b>

Table 2: The average clustering performance of ten runs on six benchmark datasets. The performance is evaluated by four metrics with mean value and standard deviation. The red and blue values indicate the best and the runner-up results, respectively.

# Experiments

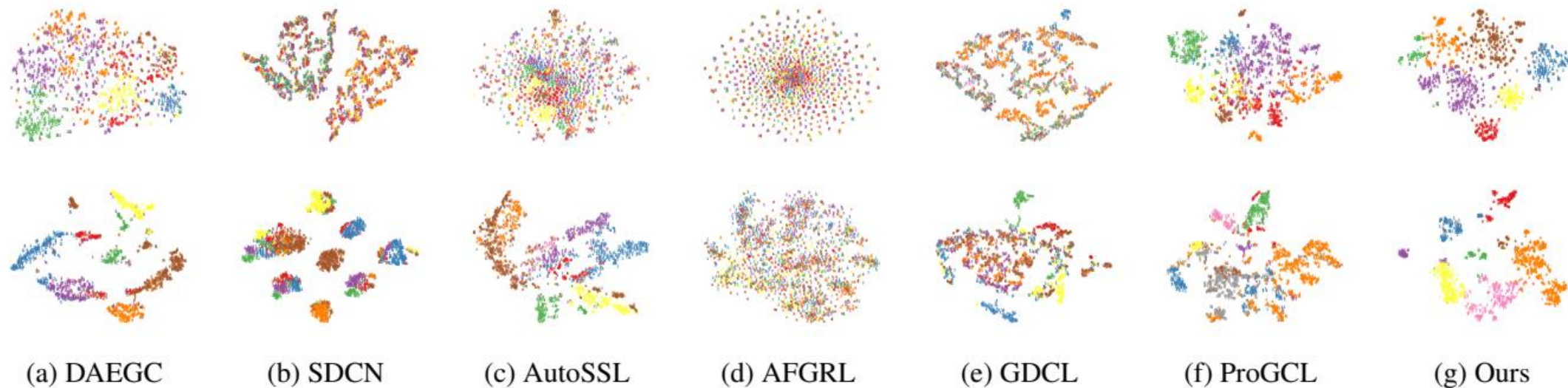


Figure 3: 2D  $t$ -SNE visualization of seven methods on two benchmark datasets. The first row and second row corresponds to CORA and AMAP dataset, respectively.



# Experiments

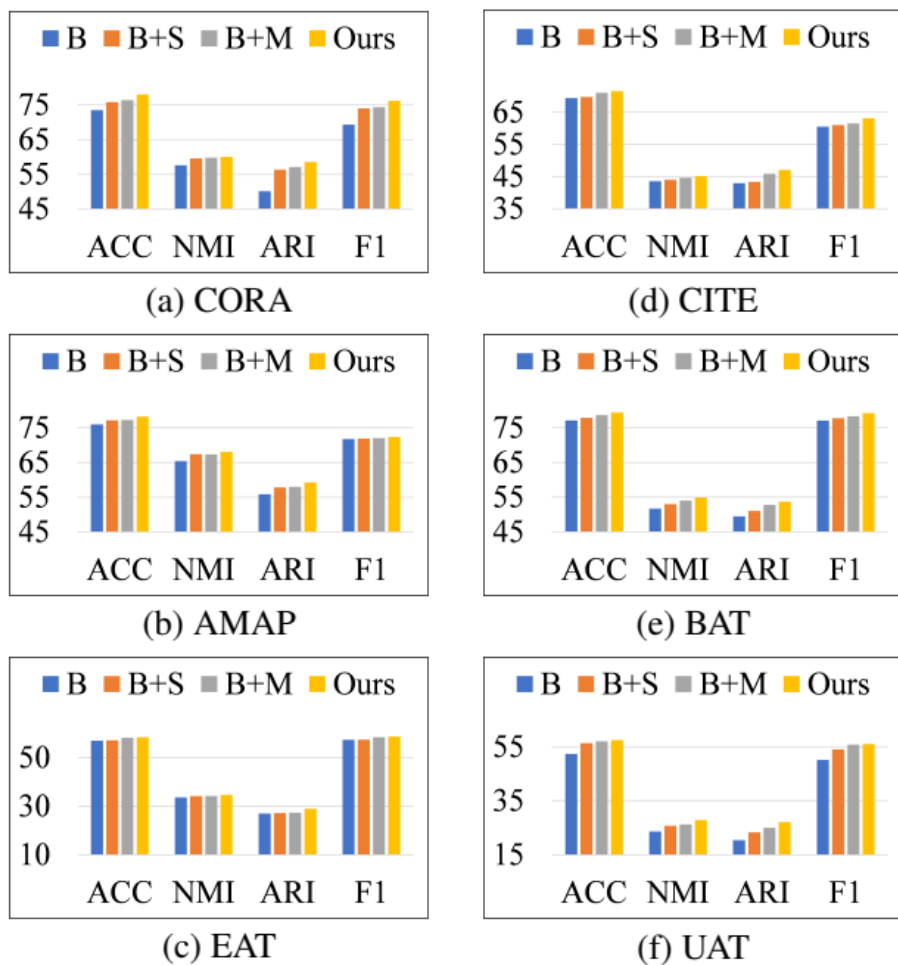


Figure 4: Ablation studies of the proposed similarity function  $\mathcal{S}$  and weight modulating function  $\mathcal{M}$  on six datasets.

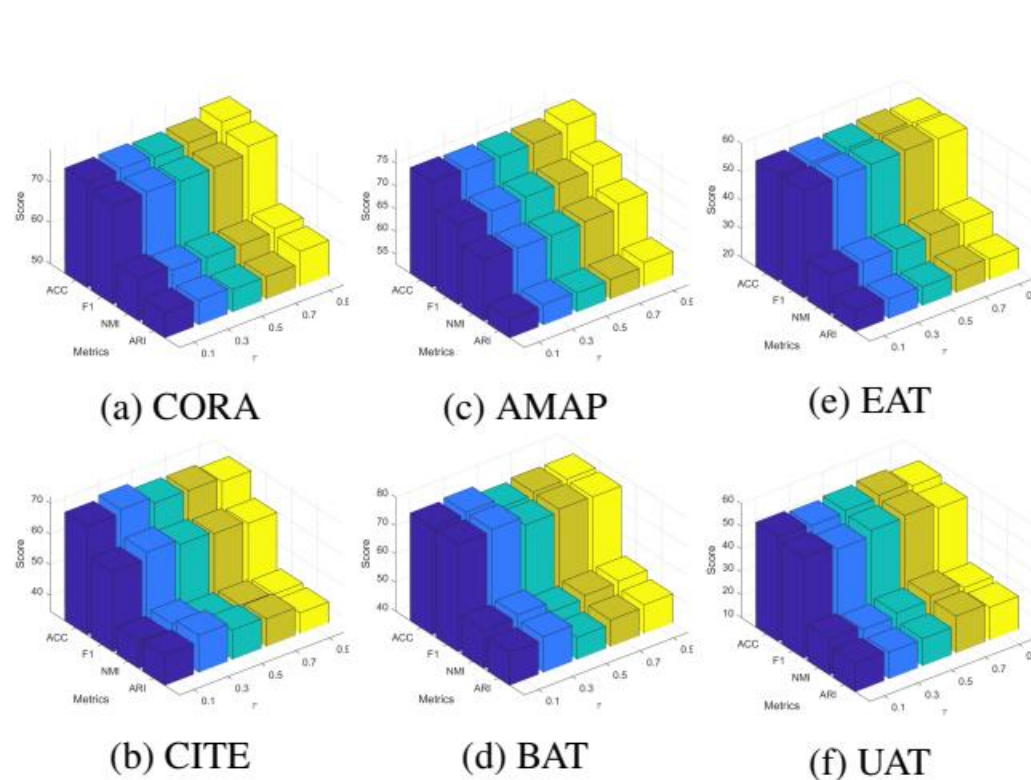
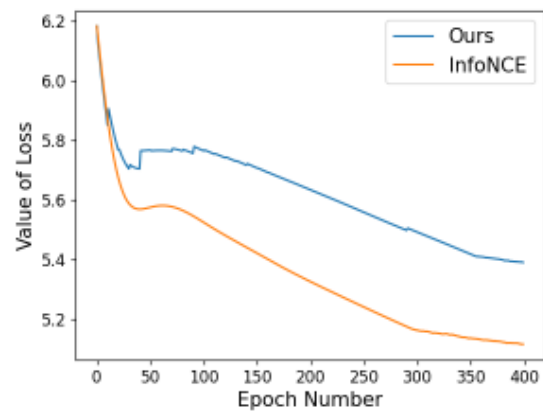
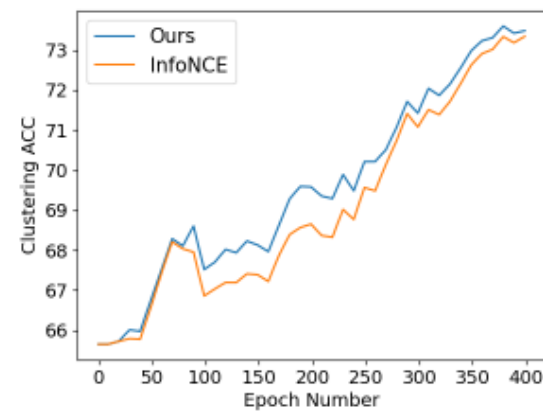


Figure 5: Analysis of the confidence hyper-parameter  $\tau$ .

# Experiments



(a) Loss on BAT



(b) ACC on BAT

Figure 6: Convergence analysis on BAT dataset.



# Thanks